Science of the Total Environment 688 (2019) 867–879

Contents lists available at ScienceDirect

Science of the Total Environment

journal homepage: www.elsevier.com/locate/scitotenv

Alternate succession of aggregate-forming cyanobacterial genera correlated with their attached bacteria by co-pathways

Cong-Min Zhu [a], Jun-Yi Zhang [b,c], Rui Guan [b], Lauren Hale [d], Ning Chen [a], Ming Li [e], Zu-Hong Lu [b], Qin-Yu Ge [b], Yun-Feng Yang [f], Ji-Zhong Zhou [d,f,g,h], Ting Chen [i,j,*]

[a] MOE Key Laboratory of Bioinformatics, Bioinformatics Division, Center for Synthetic & Systems Biology, Beijing National Research Center for Information Science and Technology, Department of Automation, Tsinghua University, Beijing 100084, China
[b] State Key Lab for Bioelectronics, School of Biological Science and Medical Engineering, Southeast University, Nanjing, China
[c] Wuxi Environmental Monitoring Centre, Wuxi, China
[d] Institute for Environmental Genomics, Department of Microbiology and Plant Biology, University of Oklahoma, Norman, OK, USA
[e] College of Resources and Environment, Northwest A & F University, Yangling, People's Republic of China
[f] State Key Joint Laboratory of Environment Simulation and Pollution Control, School of Environment, Tsinghua University, Beijing, China
[g] School of Civil Engineering and Environmental Sciences, University of Oklahoma, Norman, OK, USA
[h] Earth Sciences Division, Lawrence Berkeley National Laboratory, Berkeley, CA, USA
[i] Institute for Artificial Intelligence, Department of Computer Science and Technology, Tsinghua University, Beijing 100084, China
[j] Tsinghua-Fuzhou Institute for Data Technology, Beijing National Research Center for Information Science and Technology, Tsinghua University, Beijing 100084, China

HIGHLIGHTS

- Analyzed the taxonomic and functional composition of CAs covering a blooming cycle
- Observed *Microcystis* and *Dolichospermum* alternately dominating CAs
- Found the specific bacterial genera attached to different cyanobacterial genera
- Detected bacteria in CAs more correlated to cyanobacteria than environments
- Proved relationship between cyanobacteria and bacteria at taxonomic and gene level

GRAPHICAL ABSTRACT

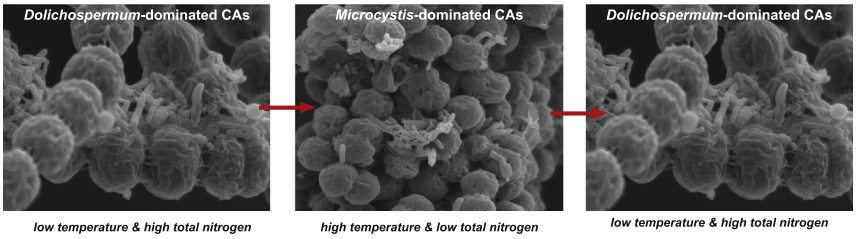

ARTICLE INFO

Article history:
Received 12 May 2019
Accepted 10 June 2019
Available online 21 June 2019

Editor: Ewa Korzeniewska

Keywords:
Cyanobacterial aggregates
Microcystis
Dolichospermum
Attached bacteria

ABSTRACT

Freshwater lakes are threatened by harmful blooms characterized by Cyanobacterial Aggregates (CAs) that are normally aggregated with extracellular polysaccharides released by cyanobacteria to form a phycosphere. It is possible that mutualistic relationships exist between bacteria and cyanobacteria in these CAs wherein bacterial products supplement cyanobacterial growth, and cyanobacterial exudates, in turn, serve as substrates for bacteria, thus augmenting the stability of each constituent. However, little is known about the exact interaction between cyanobacteria and their attached bacteria in CAs. Therefore, in this study, we collected 26 CA samples from Lake Taihu, a large freshwater lake in China from March of 2015 to February of 2016. We then sequenced both the V4 regions of 16S rRNA genes and full metagenomes, resulting in 610 Mb of 16S rRNA gene data and 198.98 Gb of high-quality metagenomic data. We observed that two cyanobacteria genera (*Microcystis* and *Dolichospermum*) alternately dominated CAs along the sampling time and specific bacterial genera attached to different cyanobacteria genera dominated CAs. More specifically, *Dolichospermum* dominates CAs when water

* Corresponding author at: Institute for Artificial Intelligence, Department of Computer Science and Technology, Tsinghua University, Beijing 100084, China.
E-mail address: tingchen@mail.tsinghua.edu.cn (T. Chen).

https://doi.org/10.1016/j.scitotenv.2019.06.150

Alternate succession
Nitrogen co-pathway

temperature is low and total nitrogen is high, while *Microcystis* dominates CAs when water temperature is high and total nitrogen is low. Moreover, we found specific bacterial genera attached to different cyanobacteria genera dominated CAs. The cyanobacteria-bacteria related pairs *Dolichospermum-Burkholderia* and *Microcystis-Hyphomonas* were detected by ecological networks construction. Bacterial communities in CAs were found to be more correlated with the cyanobacterial community (Mantel's r = 0.76, $P = 0.001$) than with environmental factors (Mantel's r = 0.27, $P = 0.017$). A potential codependent nitrogen-cycling pathway between cyanobacteria and their attached bacteria was constructed, indicating their functional link. Overall, these results demonstrated that mutualistic relationships do, indeed, exist between cyanobacteria and bacteria in CAs at both taxonomic and gene levels, providing biological clues potentially leading to the control of blooms by interventional strategies to disrupt bacteria-cyanobacteria relationships and co-pathways.

1. Introduction

Eutrophication brings with it significant economic and ecological consequences for freshwater and marine environments worldwide, including Lake Victoria in Africa (Bbosa and Oyoo, 2013), Lake Erie in North America (Mou et al., 2013), the Baltic Sea in Europe (Andersson et al., 2010), Lake Dianchi (Wu et al., 2014) and Lake Taihu in China (Guo, 2007). It has increasingly caused Cyanobacterial Harmful Algal Blooms (CyanoHABs) in freshwater systems. The frequent and extensive occurrence of large CyanoHABs on the surfaces of freshwater lakes has greatly increased the operational costs for water treatment plants and residents' concerns over cyanobacterial toxins in their drinking water supplies (Paerl et al., 2014; Paerl and Huisman, 2008). Meanwhile, owing to population growth, rapid urbanization, increased farming and climate change, the world is facing a severe shortage of fresh water, which calls for the urgent development of effective measures to prevent and treat CyanoHABs. Unfortunately, our limited understanding of CyanoHABs has impaired the development of an effective solution to prevent cyanobacterial blooms. Therefore, probing the cellular and molecular mechanisms underlying CyanoHABs would mark a critical step towards the development of preventive measures and solutions.

Most research on CyanoHABs has been focused on community composition analyses (Cai et al., 2013b; Kara et al., 2013; Otten and Paerl, 2011), related environmental factors (Beversdorf et al., 2013; Davis et al., 2009; Zhang et al., 2012) and health effects on human or other animals (Cheung et al., 2013; Fernández et al., 2015b). Cyanobacterial Aggregates (CAs) were reported as the major form of cyanobacteria during their blooms (Havens, 2008; Worm and Søndergaard, 1998) and *Microcystis* was shown to dominate the CAs in many freshwater lakes during summer (Wu et al., 2010b). In CAs, microbes were amassed within extracellular polysaccharides released by cyanobacteria, forming a phycosphere. It was hypothesized that cyanobacteria provide energy for their attached microbes *via* excreted rich extracellular organic matter, while, in turn, attached bacteria supply nitrogen, phosphorous and trace elements to cyanobacteria (Grant et al., 2014; Shi et al., 2012b). This hypothesis remains to be experimentally tested.

Metagenomic analysis has revealed novel microbe-environment interactions in humans (Falony et al., 2016; Zhernakova et al., 2016), soil (Hultman et al., 2015; Rondon et al., 2000), marine life (Lima-Mendez et al., 2015; Sunagawa et al., 2015) and many others (Tyson et al., 2004), thus serving as a powerful and convenient tool. Functional and taxonomic annotation from molecular approaches of water-borne microbial communities has enabled important breakthroughs for many freshwater lakes (Liu et al., 2014; Niu et al., 2011). However, few metagenomic studies have focused on CAs where cyanobacteria and bacteria coexist in close contact. Thus, potential metabolic links between these constituents remain unclear, preventing a mechanistic understanding of CyanoHABs (Berg et al., 2009; Cai et al., 2014). Although mutualistic relationships have been hypothesized in previous studies, little is known at the molecular level to substantiate this. However, direct sequencing of hypervariable regions of 16S rRNA genes is a convenient approach to profile the phylogenetic composition of a microbial community, and at the same time, sequence and analyze all genetic materials that can reveal potential functional links among microbial communities in CAs (Wooley et al., 2010).

Lake Taihu is the third largest freshwater lake in China irrigating millions of hectares of grains and supplying drinking water for over 2 million citizens (Qin et al., 2007). However, since the beginning of the twentieth century, CyanoHABs have been a frequent occurrence in Lake Taihu and accelerated in frequency and intensity during the last three decades by excessive nutrient loadings (Qin et al., 2007; Wang and Chen, 2008). Recently, the blooming regions have spread from bays to the lake's center, and blooming time has also expanded (Chen et al., 2003a; Hai et al., 2010). The serious consequences of CyanoHAB in Lake Taihu have resulted in increased demands for more research to supply effective measures for treatment and prevention.

CAs are the main organization of cyanobacteria during their blooms and provide a suitable and stable microenvironment wherein diverse bacteria can thrive (Tang et al., 2009). Therefore, we focused on CA communities and examined aggregates during cyanobacterial blooms to reveal the roles of cyanobacteria and their attached bacteria in CyanoHABs. To accomplish this, we collected 26 CA samples from Lake Taihu and then sequenced both 16S rRNA genes and full metagenomes for taxonomic and functional analysis at different cyanobacterial blooming stages. In this report, we asked if 1) cyanobacteria-bacteria communities in CAs of Lake Taihu show alternate succession along the time course of annual blooms, 2) attached bacteria in CAs are more correlated with the cyanobacteria community or environmental factors, and 3) a functional metabolic link exists between cyanobacteria and their closely attached bacteria. To answer these questions, we combined macro-observation of *in vivo* monitoring with microanalysis of 16S rRNA gene analysis and metagenomics.

2. Material and methods

2.1. Sample collection and site geochemistry

From March 4, 2015 to February 24, 2016, a total of 26 CA samples covering the yearly cycle of a CyanoHAB were collected from Lake Taihu. These samples were collected using monthly or weekly time-series (Table S1). The dominant cyanobacterial genera in Lake Taihu were reported as *Microcystis*, *Dolichospermum* and *Synechococcus* (Chen et al., 2003b; Ye et al., 2011). However, only *Microcystis* and *Dolichospermum* formed large-size aggregates and blooms in Lake Taihu (Shi et al., 2012a; Wang et al., 2013; Ying et al., 2015), while *Synechococcus* exists as single cells (Callieri et al., 2011). Previous studies have shown that aggregates of *Microcystis* and *Dolichospermum* in Lake Taihu were generally larger than 50 μm (Brookes et al., 1999; Smith and Gilbert, 2010; Zhu et al., 2016). In our study, we validated that the size of CAs were larger than 50 μm by examining random CAs using microscope (Fig. S1). In our experiment, we used 40 μm Cell Strainers (BD Falcon) to collect aggregate-forming CAs. During sampling, water at a depth of 0.5 m was first collected with a 5 L Schindler

sampler and then filtered through the Cell Strainers. Samples were kept motionless until most CAs had floated to the surface. Aggregates were then collected by micropipetting into tubes. To remove free-living bacteria, the samples were treated according to a vortex and washing method, which was proposed to analyze the attached microbial community on cyanobacterial aggregates (Cai et al., 2013a). We adopted the vortex and washing method with new parameters, which were validated by numerous experiments to remove as much free-living bacteria as possible and maintain cellular contents of cyanobacterial aggregates. Briefly, the tube added with ddH_2O was vortexed for 1 min and then centrifuged at 2500 $\times g$ for 15 min to obtain a thin layer of the concentrated cyanobacterial aggregates at the top surface. This layer was carefully transferred to another centrifuge tube. This vortex and washing procedure was repeated 10 times. About 10 mL of wet CAs were transferred to sterile Eppendorf tubes and stored at −80 °C for DNA extraction. Additionally, two special samples were collected to validate that the vortex and washing procedure was able to effectively remove free-living bacteria (Supplementary text). A CA-lake water mixing sample (160127.Mix) containing both CA and its surrounding lake water, and a CA sample without vortex and washing (160127.Esc) were collected and compared with the normal CA sample (160127). The CA-lake water mixture was collected and then randomly divided into three equal parts. The first part was CA-lake water mixing sample (160127.Mix). The second part was filtered through 40 μm Cell Strainers and resulted as the CA sample escaping washing preprocess (160127.Esc). The third part was firstly filtered through 40 μm Cell Strainers and then processed with vortex and washing procedure, resulted as the normal CA sample (160127).

Fifteen physicochemical factors of related CA samples were measured and recorded (Table S2). Water temperature (WT), pH, Clarity (SD), Turbidity (TURB), suspended solids (SS), dissolved oxygen (DO) and cyanobacterial cell density (ACD) were measured at positions where samples were collected with a YSI 6600 Multi-Parameter Water Quality Sonde (Ding and Zhang, 2011). One liter of water was collected from a depth of 0.5 m and used for analyses. Total nitrogen (TN), ammonium (NH_4-N), total phosphorus (TP), Permanganate Index (COD_{Mn}), biological oxygen demand (BOD), chemical oxygen demand (COD) and Chlorophyll *a* (Chla) were measured according to the standard methods of water analysis (State Environmental Protection Administration of China, 2002; Zhang et al., 2017). Water level (WL) was also recorded. Since these environmental factors are not independent from each other, we analyzed the inter-correlations among these 15 environmental factors with Spearman's correlation, resulting in eight independent factors transformed to z-scores for the correlation analysis with the composition of *CA*.

We also used remote sensing methods to monitor the CyanoHABs in Lake Taihu to provide real-time monitoring of the blooming. The remote sensing image data of Lake Taihu was collected from a NASA MODIS sensor, which features the new Earth Observation System (EOS) and has been widely used in remote sensing data collection (Salomonson et al., 1989; Shi et al., 2017). The system can receive satellite images on multiple bands with high time resolution. Collected MODIS data were analyzed by ENVI (Environment for Visualizing Images, version 4.2), a software program built to extract models of cyanobacterial bloom based on the ground object spectral theory (Kiage and Walker, 2009). We extracted the image information and calculated the affected area of cyanobacterial blooming in Lake Taihu. Finally, we summarized the pattern of cyanobacterial blooms in a year by combining the NDVI values produced by ENVI software and the visual interpretation results.

2.2. Semi-quantitative in vivo monitoring of CAs

To identify cyanobacteria responsible for the bloom, we identified the cyanobacterial constituents of CAs under an optical microscope based on morphology and estimated their relative abundance with a semi-quantitative *in vivo* monitoring method (Zhu et al., 2011). First, the CA sample was shaken into a uniform state, and 0.1 mL of the sample was transferred to a 0.1 mL counter box. Then, cyanobacteria were identified with a Nikon E1000 optical microscope at 10 × 10. To this end, 30 particles were randomly selected for species counting according to the specific population shapes.

2.3. DNA extraction and high-throughput sequencing

To extract DNA from CAs, 200 mg of CAs were first lysed by guanidine thiocyanate and N-lauroyl sarcosine (SIGMA) and then incubated in 70 °C for 1 h, followed by vortexing with beads and centrifugation. The supernatant was transferred into a new tube with 500 μl of extraction buffer (TENP mixture, including ddH_2O, Tris-HCl, EDTA, NaC, PVPP and water), vortexed and centrifuged before 500 μl supernatant were collected. This step was repeated three times. All supernatants were then centrifuged at 13,000*g* for 10 min, and the resulting supernatant was precipitated with isopropanol overnight at 4 °C. The mixture was then centrifuged at 13,000*g* for 15 min, and the supernatant was discarded. The pellet was chilled on ice for several hours after the addition of phosphate buffer and potassium acetate. Two volumes of ethyl alcohol and 0.1 volume of sodium acetate were added to the mixture, which was then stored at −20 °C for several hours. The mixture was centrifuged at 14,000*g* for 20 min, and the DNA deposit was washed twice with 70% ethanol. DNA was dissolved and preserved in TE buffer (Thermo Fisher, US).

We amplified the V4 region (250 bp) of the 16S rRNA gene to assess the taxonomic composition of the CAs. PCR conditions and primer sequences were performed as previously described (Yao et al., 2016). The purified amplicons were sequenced on an Illumina MiSeq PE250 sequencer at the Beijing Genomics Institute, Shenzhen, China (BGI). The sequence data have been submitted to the Sequence Read Archive (Accession number SRP129864).

The metagenome DNA libraries were constructed with 2 μg of DNA genomes, according to the **Illumina** TruSeq DNA Sample Prep v2 Guide, with an average of 350 bp insert size. The quality of all libraries was evaluated using an Agilent bioanalyzer with a DNA LabChip 1000 kit. All qualified libraries were loaded to Illumina HiSeq2500 to be sequenced at BGI. The sequenced reads were deposited in the Sequence Read Archive (Accession number SRP129300).

2.4. 16S rRNA gene sequence data processing

The 16S rRNA genes of 25 CA samples were sequenced, and raw data generated were analyzed using Quantitative Insights into Microbial Ecology (QIIME) (Caporaso et al., 2010). In brief, sequences were demultiplexed based on a unique barcode assigned to each sample. Sequences with quality scores lower than 20 and length shorter than 200 were filtered out. Then Operational Taxonomic Units (OTUs) were identified using an open-reference OTU picking protocol at a 97% similarity cutoff. We mapped the OTUs to the Greengenes database (V201305) (Desantis et al., 2006) to identify their taxonomy, and removed OTUs without alignment results. We estimated raw abundance of OTUs in each sample by counting the read numbers and conducted diversity analyses. After obtaining the OTU tables and phylogenetic trees, we calculated microbial richness estimators (Observed OTUs, PD whole tree and Chao1), evenness estimators (Equitability), and diversity estimators (Simpson Index) by using the R statistical calculation software package 'vegan' (O'Hara et al., 2011; Simpson et al., 2015). To generate rarefaction curves, we randomly selected a fixed number of sequences from each dataset, using the lowest read number in our samples (~25 k sequences) to rarify the OTU abundance data. For beta-diversity analysis, we estimated weighted uniFrac distances based on the OTU tables and the phylogenetic trees.

We calculated uniFrac distances of composition of CAs between samples, Euclidean distances of environmental factors between

samples, and Vincenty distances of geography between samples. To identify environmental drivers independent of geographic distance, we computed distance-corrected correlations between CA composition and environmental factors by partial Mantel test using the R package 'vegan' with 9999 permutations. In order to determine whether cyanobacteria of CAs were more correlated with environment or bacteria, we first computed the geographic distance (G) and then the bacterial community (B) corrected partial Mantel correlations (R(C,E|G,B)) between cyanobacterial composition (C) and environmental factors (E). Next, we computed the geographic distance and environment-corrected partial Mantel correlations between cyanobacterial composition and bacterial composition (R(C,B|G,E)). Finally, we compared Mantel's r and *P*-value from these two Mantel tests (R(C,E|G,B) and R (C,B|G,E)). To determine whether the bacteria in CAs were more correlated with the environment or cyanobacteria, we also computed the geographic distance and cyanobacterial community-corrected partial Mantel correlations between bacterial composition and the environment (R(B,E|G,C)). We then compared R(B,E|G,C) with the correlations between cyanobacterial composition and bacterial composition (R(C, B|G,E)). Structural equation modeling (SEM) was used to explore how environmental variables were integrated with and affected by cyanobacteria and bacteria. We first considered a full model that included all possible pathways and then sequentially eliminated non-significant pathways one-by-one until we generated the final model where all pathways were significant. We used the χ^2 test and the root mean square error to evaluate how well the model fits. The SEM-related analysis was performed using the R package 'lavaan (Rosseel, 2015)'.

2.5. Metagenomic data processing

Illumina raw reads were filtered with the following constraints: (1) reads with >2 ambiguous N bases were removed; (2) reads with <80% of high-quality bases (Phred score ≥20) were removed; (3) 3′-ends of reads were trimmed to the first high-quality base. Then, filtered metagenomic reads were assembled by Megahit (version 1.0.5) (Li et al., 2015) into contigs in a time- and cost-efficient way, using the following parameters: –min-contig-len = 150, –k-min = 27, –k-max = 123, –k-step = 8 and –min-count = 1. All assembled contigs were submitted to MetaProdigal (version 2.6.3) (Hyatt et al., 2012) for gene calling using the default parameters. We aligned all reads to genes by Bowtie2 and calculated the gene coverage using bedtools (version 2.26) (Quinlan and Hall, 2010). We mapped the predicted genes to NCBI bacteria, archaebacterial and virus non-redundant genome databases by Diamond (Buchfink et al., 2015). The alignment result was then submitted to Megan (version 6) (Huson et al., 2007) to estimate the taxonomic and functional compositions with weighted LCA algorithm. The taxonomic analysis was performed with NCBI bacterial, **archaeal** and viral non-redundant genome databases. The functional analysis was conducted by mapping genes to Kyoto Encyclopedia of Genes and Genomes (KEGG) (Kanehisa et al., 2004) and SEED (Overbeek et al., 2005).

To identify novel genomes from metagenomic sequencing data, we used CONCOCT (version 0.4.1) (Alneberg et al., 2014) to cluster all contigs longer than 1 Kb from all samples into draft genomes (called bins) based on sequence compositions and coverages across multiple samples with default parameters. We set the maximum cluster number to 300. Then, we applied CheckM (version 1.0.6) (Parks et al., 2015) to estimate the completeness and contamination for each bin. Finally, the bins with high completeness (>70%) and fewer contaminants (<10%) were retained as draft genomes. The draft genomes were annotated by mapping to NCBI bacterial, archaeal and viral non-redundant genome databases using a program called Diamond. Their functional compositions were estimated based on KEGG mapping results using MEGAN (MEtaGenome ANalyzer) software.

2.6. Comparative analysis between DCA and MCA

2.6.1. Sample grouping

According to semi-quantitative *in vivo* monitoring results of CA samples, two cyanobacterial genera, *Dolichospermum* and *Microcystis*, alternately dominated the CA samples from March of 2015 to January of 2016, with the dominant CAs shifting from *Dolichospermum* genus to *Microcystis* genus in early May and back to *Dolichospermum* genus again at the end of December. Therefore, we partitioned the 26 CA samples into two groups as shown in Table 1, DCA (*Dolichospermum*-dominated CAs) and MCA (*Microcystis*-dominated CAs), using the k-mean clustering method (Kanungo et al., 2002). We applied the same clustering method to the environmental factors to validate accuracy of our sample grouping.

2.6.2. Taxonomic and network comparative analyses

We compared the 16S rRNA gene-based taxonomic abundance of *Dolichospermum* and *Microcystis* in DCA with that in MCA. Differences in the relative abundance of bacteria in DCA and MCA were analyzed using Wilcoxon rank-sum test. Difference in alpha diversity (α-**diversity**) of the two groups was also compared. *P*-values < 0.05 were used to indicate statistical significance. We estimated the copy number of the rRNA operon for each OTU based on its closest relatives with known rRNA operon copy number (Wu et al., 2017) in the rrnDB database (Stoddard et al., 2015). For an OTU without copy number information, we assigned it with the operon copy number of its parent taxon. For OTUs with copy number data, we calculated the mean operon copy number of its immediate child taxa. The abundance-weighted average rRNA operon copy number of each sample was then estimated by taking the product of the estimated operon copy number and the relative abundance of each OTU and summing this value across all OTUs in a sample. The abundance-weighted average rRNA operon copy number for samples between DCA and MCA was compared by Wilcoxon rank-sum test.

To compare the ecological network between DCA and MCA, we first constructed networks respectively for DCA and MCA by Molecular Ecological Network Analyses (MENA) (Deng et al., 2012; Zhou et al., 2010; Zhou et al., 2011), which calculated the Pearson correlation coefficients (PCC) for each pair of OTUs, and then used the permutation test to compute the statistical significance of the PCC value. Edges were set between pairs of OTUs for which the PCC was significant (FDR < 0.01). Then, we calculated and compared the network topology characteristics of these two networks using the Network Analyzer plugin in Cytoscope (Assenov et al., 2007).

Table 1
Grouping CA samples according to semiquantitative *in vivo* monitoring results.

MCA		DCA	
Sample ID	*Microcystis* (%)	Sample ID	*Microcystis* (%)
150504	69.9	150304.1	21.4
150514.1	97.3	150304.2	50
150514.2	89.7	150306	12.2
150521	96.4	150402	40
150608.1	88.5	150409.1	55.2
150608.2	97.2	150409.2	50.7
150615	98.9	150420	60.6
150701	98.8	150427	52.9
150804	100	160104	10.0
150806	99.2	160119	5.9
150902	99.5	160127	14.7
151028	89.3		
151123	100		
151211	99.1		
151222	77.9		

2.6.3. Functional comparative analyses

Differentially abundant pathways were detected by performing KEGG Ontology (KO) enrichment analysis with Gene Set Enrichment Analysis (GSEA) (V2-3.0_beta_2) (Mootha et al., 2003; Subramanian et al., 2005). To this end, we treated the gene abundance table annotated with KEGG as input of the GSEA and KEGG pathway file, which contained pathway names and genes involved in each pathway. We defined the significance with FDR *P*-value < 0.05 to find the pathways with significant abundance in DCA and MCA. Since different pathways may share same genes, we measured the relationship between those significant pathways by combining Jaccard distance and number of overlapping genes, each with weight of 0.5. We set the threshold of 0.35 to obtain a relationship network between those pathways.

2.6.4. Nitrogen metabolism analyses

Wilcoxon rank-sum test was performed to compare the relative abundance of genes involved in nitrogen metabolism. *P*-value < 0.05 was used to determine genes with significant abundance in DCA and MCA. To test whether nitrogen metabolism is a functional link between cyanobacteria and their attached bacteria, we mapped genes in each CA sample to KEGG nitrogen metabolism (map00910) to identify the modules of nitrogen cycle. Then, we downloaded reference genomes of *Microcystis* and *Dolichospermum* from NCBI's Genomes Resource and mapped them to KEGG nitrogen metabolism to detect the modules of nitrogen cycle respectively in *Microcystis* and *Dolichospermum*. To find other participants in the nitrogen cycle, we mapped the draft genomes binned from metagenomic sequencing data to KEGG nitrogen metabolism to check whether these genomes contain genes associated with the nitrogen cycle.

3. Results

3.1. Data description and metadata analysis

From March 2015 to January 2016, we collected 26 CAs from the northern bays of Lake Taihu where cyanobacteria carried out a near full-year bloom cycle (Table S1). Scanning diagram of electron microscope validated the presence of both cyanobacteria and other bacteria (cocci and rods) within the CA samples (Fig. S1A–B). Scanning microscopy of four randomly selected CAs showed the large size of aggregates >50 μm (Fig. S1C–F). All samples were used in metagenome sequencing, but only 25 samples were used in 16S rRNA gene amplicon sequencing, owing to a limited amount of DNA yielded from sample 150,304.2. In total, 610 Mb of 16S rRNA gene data were generated from Illumina MiSeq sequencing, and 198.98 Gb of high-quality metagenome data were generated from Illumina HiSeq sequencing. The amount of data reached the saturation stage as shown by the rarefaction curves, and this proves that we have captured most information of the community of CAs (Fig. S2A).

Using real-time remote sensing image data of Lake Taihu, we calculated the total aggregation area of the cyanobacteria, as well as maximum area and frequency of cyanobacterial blooms per month from 2010 to 2015. The results indicated that the frequency of blooms dramatically increased over time and that the timespan of the occurrences expanded from May to October and to almost a whole year, except February (Table S2), which is consistent with previous reports (Chen et al., 2003a; Hai et al., 2010). Fifteen physicochemical factors were measured to cover the major hydrographic features (WT, pH, SD, TURB, SS and WL), index of organic pollutants (DO, BOD and COD), index of reducing matter (TN, NH_4-N and TP), permanganate Index (COD_{Mn}), and algae index (BOD and Chla) (Table S3). WT, TN and TP showed significant variation across the sampling time (Fig. S2B). WT increased first, peaked in August, and then decreased. Conversely, TN decreased first, bottomed out in November, and then increased. TP remained relatively steady until increasing in December. Spearman's correlations of these environmental factors indicated modest, or high, inter-correlations between some factors, including TP and Chla (0.52), TN and TP (0.60), and WT and TN (−0.69) (Fig. S2C). Then we clustered the samples into two groups according to these environmental factors (Fig. S3A).

3.2. Alternate succession of dominant cyanobacterial genus

Counting the aggregates of cyanobacterial genera in CA samples by the semi-quantitative *in vivo* monitoring method, we identified two cyanobacterial genera, *Dolichospermum* (Fig. 1A (a, b, f)) and *Microcystis* (Fig. 1A (c, d, e)), and their constituent species, two and eight respectively, as the dominant cyanobacteria in all CA samples with their total abundance averaging about 98% of cyanobacteria composition (Table S4). *Dolichospermum* and *Microcystis* alternately dominated the CA samples from March 2015 to January 2016, with the dominant cyanobacteria shifting from members of *Dolichospermum* to members of *Microcystis* in the early May and back to members of *Dolichospermum* again at the end of December (Fig. 1B). Specifically, *Dolichospermum* dominated the months of March, April, and January in the second year with an average relative abundance of 59%, and in other months, its average abundance was only 5.8%. *Microcystis* dominated the months from May to December with an average abundance of 93.6%, and in other months, its average abundance was 38.2%. Additionally, semi-quantitative *in vivo* monitoring results of the CA samples recorded from April 2014 to March 2016 validated alternate succession between the two dominant cyanobacteria genera that covered the whole yearly cycle of CyanoHABs (Fig. S3B). Accordingly, these 26 CA samples were partitioned into two groups: DCA (*Dolichospermum*-dominated CA) with 15 samples, and MCA (*Microcystis*-dominated CA) with 11 samples. MCA dominated the heavy blooms between May and December, while DCA dominated light blooms in other months of the year. 16S rRNA gene sequencing data analysis of cyanobacterial compositions also showed that *Microcystis* was the dominant cyanobacteria genus in 87.5% of samples from May to December, while *Dolichospermum* dominated in 90% samples in other months (Fig. S3C). The sample grouping results of DAC and MCA are about 81% consistent with the sample k-means clustering results based on environmental factors (Fig. S3A).

3.3. Taxonomic change of attached bacteria along cyanobacterial succession

16S rRNA gene amplicon sequencing data showed that the three most abundant microbial phyla in the CAs were Cyanobacteria (39.3%), Proteobacteria (33.2%) and Bacteroidetes (20.5%) (Fig. 2A). Similar results were observed in taxonomic classification of the assembled contigs from the metagenome sequencing data with correlation coefficient r > 0.85 (Fig. 2B–C). First, 4733 OTUs were shared by both MCA and DCA, but MCA contained more specific OTUs (5877) than DCA (2114). As a result, MCA had significantly higher *a*-diversity values than DCA, indicating that much more diverse bacterial communities closely attached to *Microcystis*, forming, consequently, a more complex phycosphere (Fig. 2D). We calculated the abundance-weighted average rRNA operon copy number of OTUs for each sample (Fig. 2E). Wilcoxon rank-sum test indicated that DCA showed significantly higher average rRNA operon copy number than MCA ($P = 0.0018$). Additionally, significant correlation was observed between the abundance-weighted average rRNA operon copy number and both TN (Pearson r = 0.62) and TP (Pearson r = 0.57).

To detect the specificity of the attached bacteria to different cyanobacteria genus dominated CAs, we performed Wilcoxon rank-sum test (FDR q value < 0.05 with 1000 permutations) between MCA and DCA based on the taxonomic composition of CAs, excluding *Microcystis* and *Dolichospermum* genera, resulting in 31 genera and 27 genera that were significantly enriched in the MCA and DCA groups, respectively (Fig. 1C). Nineteen out of the 31 genera were enriched in MCA and 17 out of the 27 genera were enriched in DCA belonged to the phylum Proteobacteria. The Gemmatimonadetes phylum contained

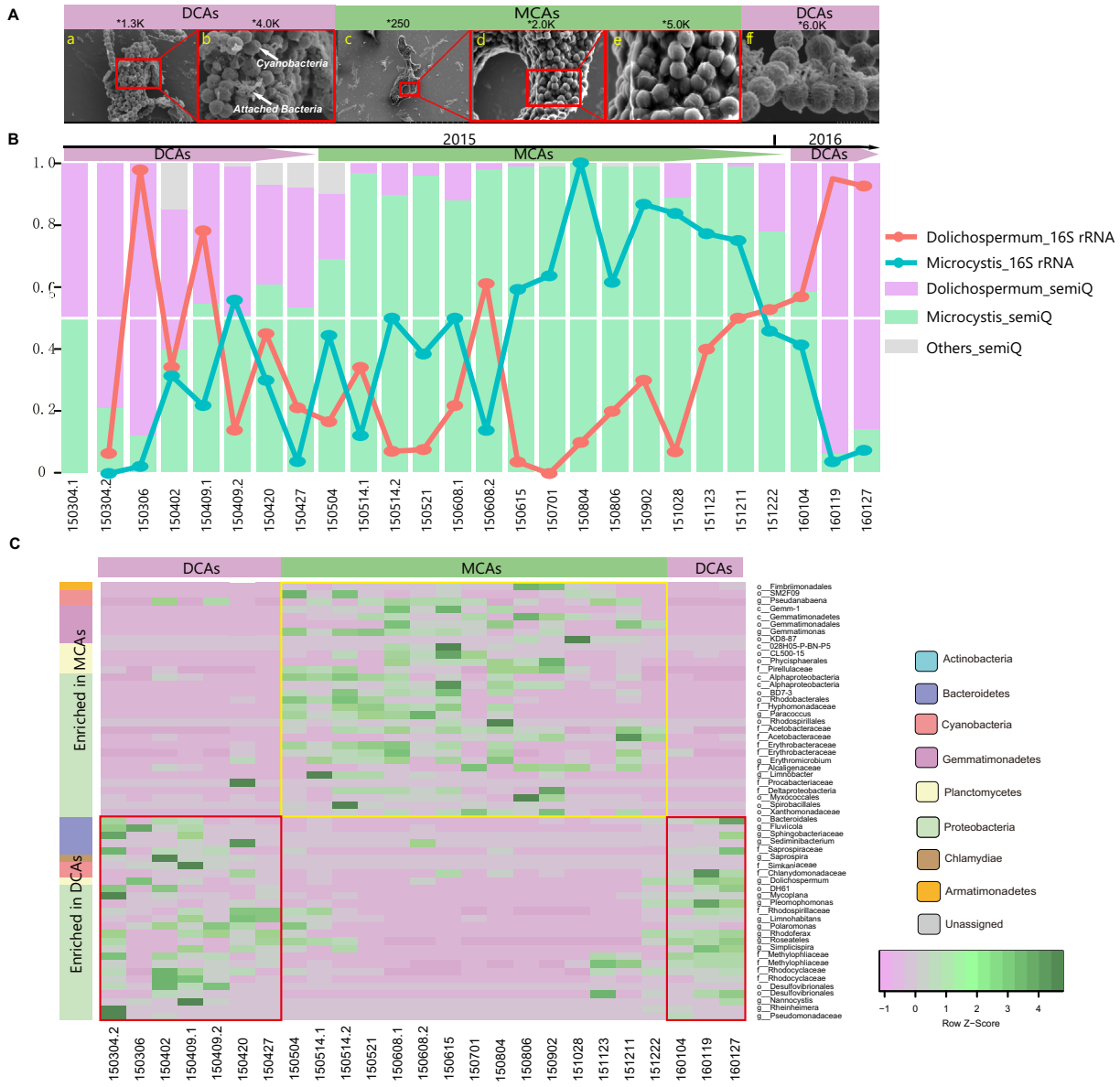

Fig. 1. Alternate succession of dominant cyanobacteria in CAs and their attached bacterial populations. (A) Different morphological features of MCA and DCA under microscopy. (a, b, f) *Dolichospermum*-dominated aggregates appear like a long chain under microscopy. (c–e) *Microcystis*-dominated aggregates appear like flakes under microscopy. (B) Alternate succession between *Dolichospermum* (red) and *Microcystis* (green), as dominant algae, based on semiquantitative *in vivo* monitoring results (bar plot) and 16S rRNA sequencing results (line plot). (C) Wilcoxon rank-sum test (P-value < 0.01) between MCA group and DCA groups based on 16S rRNA sequencing data showed that 31 genera and 27 genera are respectively significantly enriched in the MCA (in yellow box) and DCA groups (in red box). The left bar is colored with the phylum name.

5 genera enriched in MCA, and the Bacteroidetes phylum contained 6 genera enriched in DCA.

3.4. Ecological networks of microbial genera along cyanobacterial succession

We constructed ecological networks for DCA and MCA (Fig. 3A) and then analyzed their network topology characteristics (Table S5). Strikingly, both *Dolichospermum* and *Microcystis* were identified as keystone species (Fig. 3B), suggesting that they play central roles in the community. *Dolichospermum* had 11 neighbors, as detected by correlations, including 10 Proteobacteria genera and 1 Chloroflexi genus. All neighbors were positively correlated to *Dolichospermum*, except one that could be annotated as *Burkholderia*. *Microcystis* had 12 positively correlated neighbors and 5 negatively correlated neighbors, and they included 13 Proteobacteria genera, 2 Gemmatimonadetes genera, 1 Chlorobi genus, and 1 unassigned genus.

A total of 292 edges were detected for 118 genera in the DCA association network, and 307 edges for 94 genera in the MCA association network. A lower percentage of negative relationships were found in the MCA group (19.9%) than the DCA group (28.4%), suggesting that more microbes coexisted in mutualistic relationships in the MCA group. As shown in Table S5, the average clustering coefficient of the MCA network was 0.23, much larger than that of a random network of the same scale (0.056), while the characteristic path length for this network was 4.2, slightly higher than that of a random network (2.6). Similar results were obtained in the DCA network, indicating that most microbes in the networks were closely linked by a high level of dependence.

3.5. Environmental and community drivers of CA composition

To identify environmental drivers of CA composition independent of geographical distance, we correlated distance-corrected dissimilarities of community composition with distance-corrected

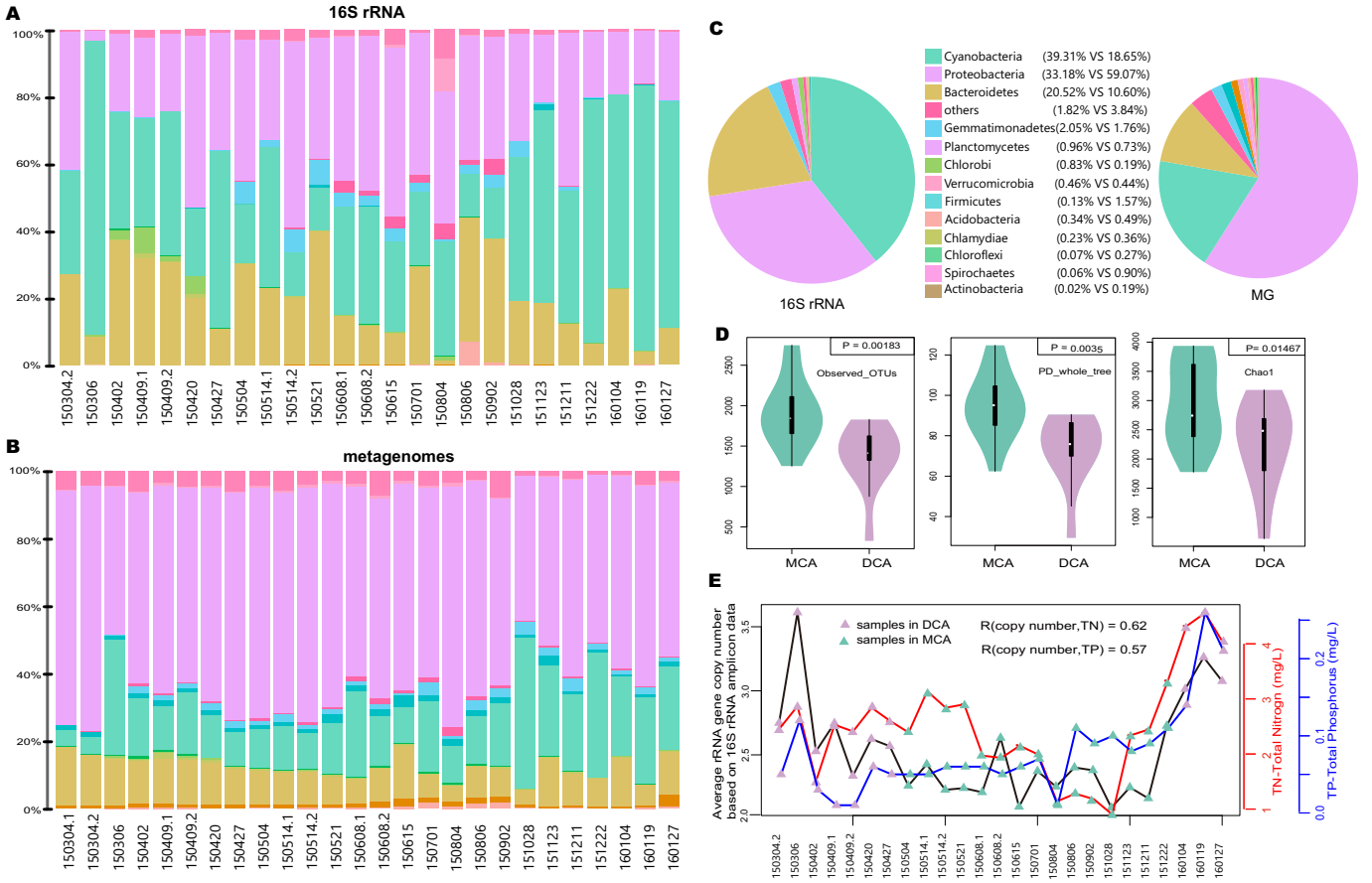

Fig. 2. Taxonomic composition of CAs and *a*-diversity comparison between two groups. (A) Composition profiling of 25 CA samples resulting from 16S rRNA amplicon sequencing data. (B) Composition profiling of 26 CA samples resulting from metagenomics data. (C) Pie plot of average composition resulting from 16S rRNA. (D) MCA shows more diversity than DCA based on two *a*-diversity indexes (Observed_OTUs, PD_whole_tree and Chao1). (E) Abundance-weighted average rRNA operon copy number of OTUs for each sample (black line). Total nitrogen for each sample (red line). Total phosphorus for each sample (blue line).

dissimilarities of major environmental factors by partial Mantel test (Fig. 4A). Overall, TP, TN, WT and DO were correlated with taxonomic compositions of CAs with Mantel's r = 0.54, 0.52, 0.47 and 0.46, respectively, while WL (Water Level), representing sampling season variation, was also strongly correlated with the functional composition of CA based on Mantel's r = 0.25. According to the dynamics of WT and TN, when WT is low and TN is high, *Dolichospermum* dominates the CAs. In contrast, when WT is high and TN is low, *Microcystis* dominates the CAs.

Furthermore, we correlated distance-corrected dissimilarities of cyanobacterial composition with distance-corrected dissimilarities of environmental factors, and with distance-corrected dissimilarities of bacterial composition by partial Mantel test. Results show that cyanobacterial composition was more closely correlated with environmental factors (Mantel's r = 0.85, $P = 0.001$) than with aggregated bacterial composition (Mantel's r = 0.76, $P = 0.001$). To compare the influence of environment factors and cyanobacterial composition on bacterial composition in CAs, we correlated the bacterial composition with environmental factors. The results show that bacterial composition was more closely correlated with cyanobacteria (Mantel's r = 0.76, $P = 0.001$) than with environmental factors (Mantel's r = 0.27, $P = 0.017$).

We applied structural equation modeling (SEM) to analyze potential mechanisms controlling bacterial *a*-diversity (Fig. 4B). The cyanobacterial *a*-diversity was found to be the most influential variable directly related to bacterial diversity (standardized path coefficient = 0.40, $P < 0.05$). The SEM result was consistent with the partial Mantel test. These results suggest that the cyanobacteria were closely correlated with environmental factors, including TP, TN and WT, and that the attached bacteria were more affected by the community composition of cyanobacteria than by environmental factors.

3.6. Pathways of flagellar assembly, cell cycle and biosynthesis of amino acids enriched in MCA

To examine functional variations among CA communities, we performed pathway enrichment analyses and detected 15 pathways significantly enriched in the MCA group compared to the DCA group (FDR q value < 0.05 with 1000 permutations) (Fig. 5 and Table 2). Flagellar assembly pathways related to bacterial movement in viscous environments were enriched in MCA group. During the cyanobacterial heavy blooms in summer and autumn, *Microcystis* spp., as the dominant algae, usually organized and formed viscous aggregates *via* secreting extracellular polysaccharides.

Other synthesis pathways were also significantly enriched in the MCA group, including those involved in cell cycle, biosynthesis of amino acids, peptidoglycan biosynthesis and lysine biosynthesis, which are associated with fast cell growth. Because these pathways share some genes, the relationship between the pathways was calculated based on the number of overlapping genes and their Euclidean distance with the threshold of 0.35. Carbon-related pathways and amino acids-related pathways were closely correlated and enriched in MCA (Fig. 5). In contrast, no pathway was enriched in DCA compared to MCA, indicating that the DCA communities were less active compared to the MCA communities. Additionally, fatty acids were more likely to be synthesized (95% probability) in the MCA group and degraded by

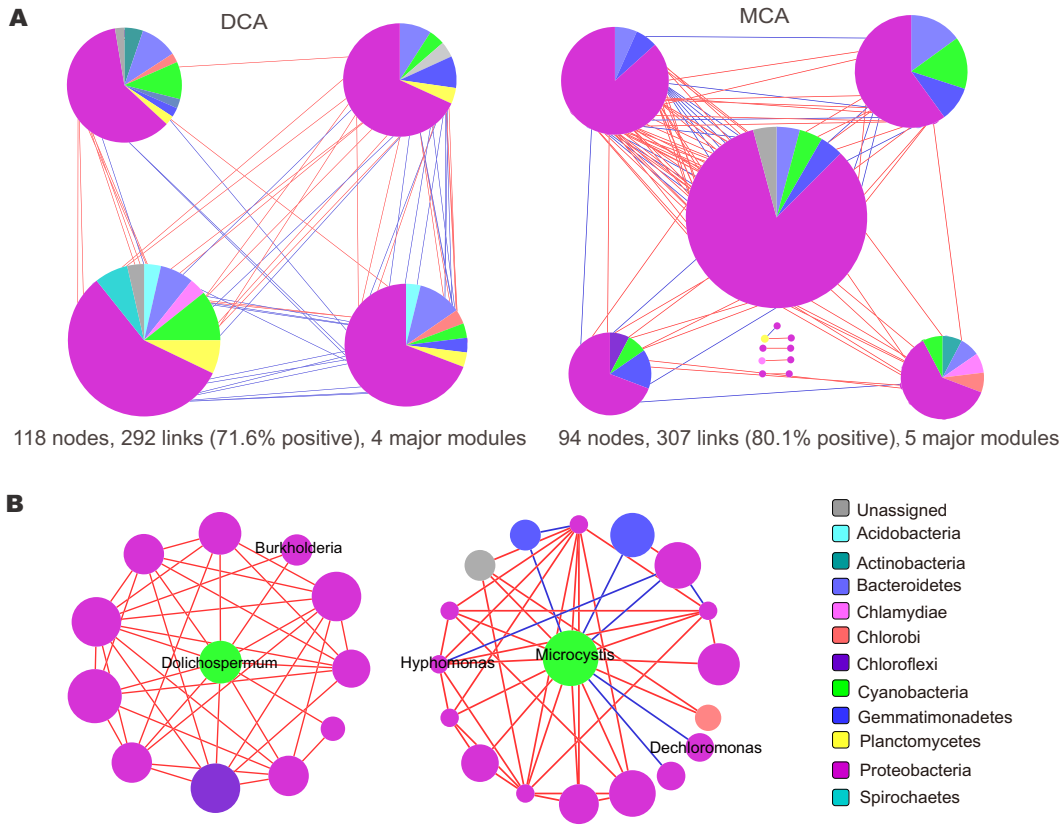

Fig. 3. Ecological networks of MCA and DCA groups. (A) Network interactions of the genera from DCA and MCA groups. Pie charts represent the composition of major modules with >10 nodes with colors indicating different phyla. A red link indicates positive covariation, whereas a blue link indicates negative covariation. (B) Bacteria correlated with *Dolichospermum* and *Microcystis*. Node colors indicate different major phyla. Size of node is proportional to the average clustering coefficient of the node.

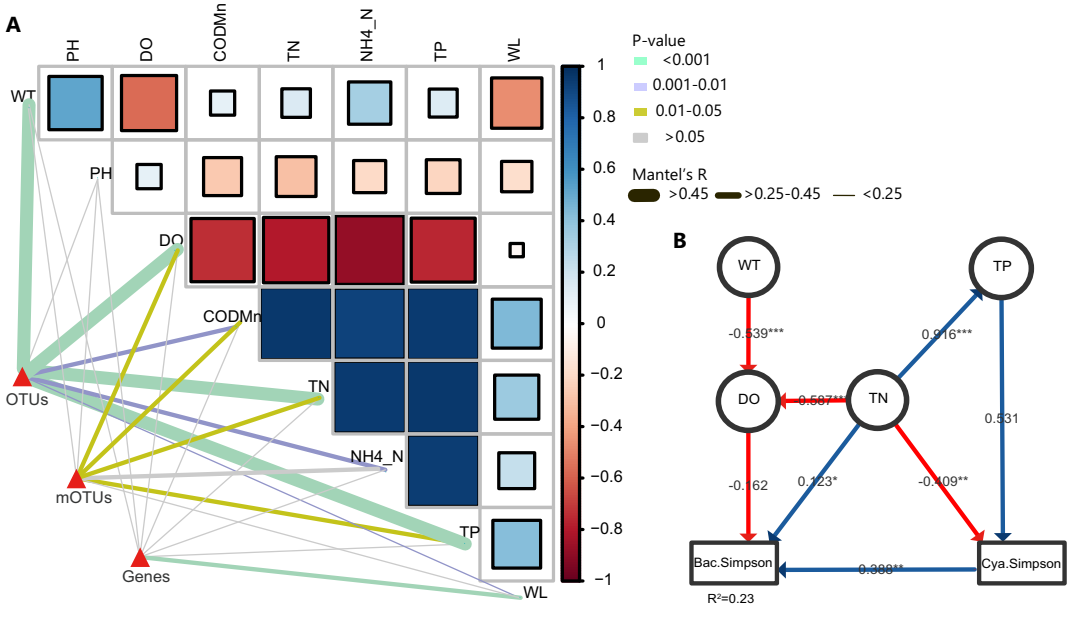

Fig. 4. Environmental drivers of microbial community and structural equation model in *CA*. (A) Environmental drivers of microbial CA community. Pairwise comparisons of environmental factors are shown with color gradient denoting Spearman's correlation coefficients. Taxonomic (OTUs resulting from 16S rRNA and mOTUs resulting from metagenomics) and functional (genes) composition in relation to 8 major environmental factors by partial (geographic distance-corrected) Mantel tests. Edge color denotes statistical significance based on 9999 permutations, and edge width corresponds to Mantel's R statistic for the corresponding distance correlations. (B) A structural equation model showing the direct and indirect effects of multiple environmental and operation variables on bacterial diversity in *CA*. Observed environmental variables are represented by circle. Composite variable represented by rectangles. Blue and red arrows represent significant positive and negative pathways, respectively. Numbers near the pathway arrow indicate the standard path coefficients. Arrow width is proportional to the strength of the relationship. Model $\chi^2 = 14.780$, df $= 8$, $P = 0.1$. The results show that bacterial diversity was more correlated to cyanobacteria than environmental factors.

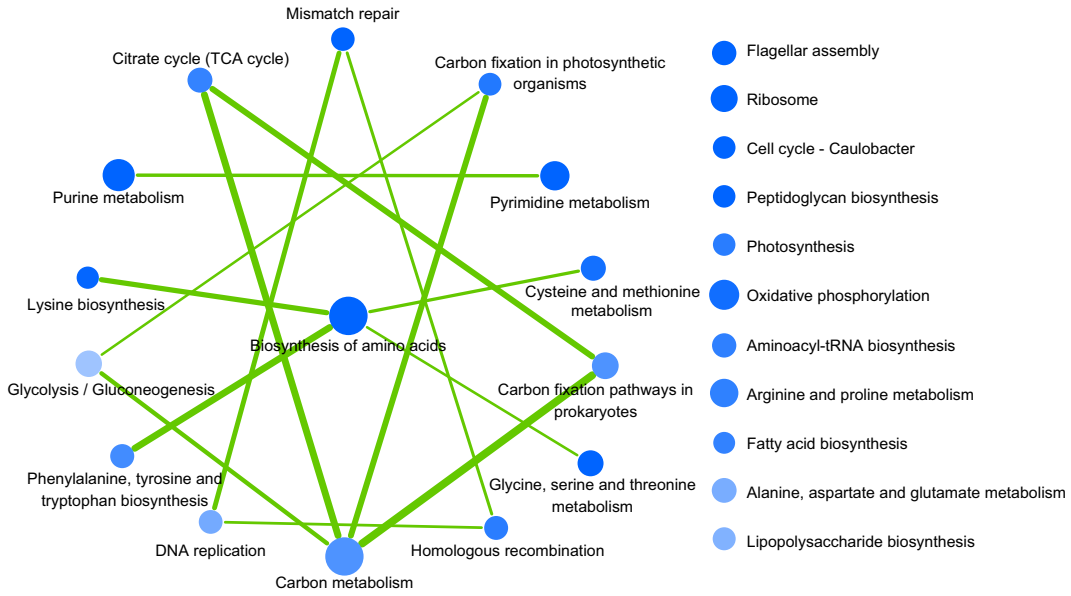

Fig. 5. The 25 most significant pathways enriched in MCA groups and their relationships. Each node is a pathway. The darker the blue color of the node, the more significantly enriched the pathway is. The size of the node is proportional to the gene number involved in the pathway. The relationship between pathways was calculated based on the number of overlapping genes and their Euclidean distance with the threshold of 0.35. The link indicates that the relationship between two nodes is bigger than 0.35 and that the width is proportional to the relationship value.

the DCA group (60% probability), potentially implying higher metabolic activity in the MCA group.

3.7. Nitrogen co-pathway between cyanobacteria and their attached bacteria

Nitrogen was detected as one of the most correlated factors with CAs, consistent with previous studies (Sommer, 1989; Vézie et al., 2002). We observed that bacteria in CAs were closely related to cyanobacterial composition, suggesting that nitrogen cycle is an important functional link between cyanobacteria and their attached bacteria. To test this hypothesis, we first identified the modules of nitrogen cycle appearing in the microbial community of all 26 CA samples by annotating the predicted gene sets with both SEED and KEGG. The core nitrogen cycle involves four reduction pathways (nitrogen fixation, assimilatory **reduction** of **nitrate** to ammonium (**ANRA**), dissimilatory

Table 2
Pathways enriched in MCA and DCA after gene set enrichment analysis.

Group	Pathway	Name	#Gene	ES	NES	NOM *p*-val	FDR *q*-val
MCA	KO02040	Flagellar assembly	35	0.64	2.52	0.0000	0.000
	KO04112	Cell cycle - Caulobacter	21	0.71	2.37	0.0000	0.0000
	KO01230	Biosynthesis of amino acids	144	0.43	2.20	0.0000	0.0017
	KO00550	Peptidoglycan biosynthesis	20	0.62	2.08	0.0000	0.0039
	KO00240	Pyrimidine metabolism	73	0.45	2.05	0.0000	0.0037
	KO00260	Glycine, serine and threonine metabolism	47	0.48	2.03	0.0000	0.0039
	KO03010	Ribosome	55	0.47	2.01	0.0000	0.0056
	KO03430	Mismatch repair	28	0.53	1.93	0.0000	0.0085
	KO00230	Purine metabolism	95	0.38	1.84	0.0000	0.0149
	KO00195	Photosynthesis	20	0.55	1.86	0.0020	0.0142
	KO00720	Carbon fixation pathways in prokaryotes	53	0.42	1.79	0.0038	0.0207
	KO01200	Carbon metabolism	143	0.31	1.59	0.0038	0.0610
	KO00300	Lysine biosynthesis	18	0.54	1.70	0.0060	0.0387
	KO00190	Oxidative phosphorylation	79	0.32	1.49	0.0092	0.0899
	KO00270	Cysteine and methionine metabolism	40	0.44	1.78	0.0098	0.0209
DCA	KO02010	ABC transporters	166	0.29	1.56	0.0000	0.4288
	KO02060	Phosphotransferase system (PTS)	23	0.44	1.51	0.0337	0.3088
	KO00071	Fatty acid degradation	23	0.38	1.33	0.1279	0.5970
	KO04146	Peroxisome	15	0.41	1.27	0.1946	0.6073
	KO00360	Phenylalanine metabolism	26	0.35	1.24	0.1714	0.5634
	KO04141	Protein processing in endoplasmic reticulum	15	0.37	1.13	0.3091	0.7860
	KO00040	Pentose and glucuronate interconversions	26	0.31	1.13	0.2860	0.6782
	KO00640	Propanoate metabolism	43	0.25	1.03	0.3931	0.8768
	KO00500	Starch and sucrose metabolism	51	0.23	0.99	0.4915	0.8976
	KO00630	Glyoxylate and dicarboxylate metabolism	45	0.24	0.98	0.4830	0.8255
	KO00052	Galactose metabolism	25	0.27	0.96	0.5072	0.7916
	KO00627	Aminobenzoate degradation	17	0.26	0.85	0.6660	0.9891
	KO00280	Valine, leucine and isoleucine degradation	32	0.22	0.83	0.7309	0.9576
	KO00340	Histidine metabolism	25	0.23	0.83	0.7065	0.9007
	KO00350	Tyrosine metabolism	21	0.22	0.76	0.8103	0.9471

reduction of nitrate to ammonium (DNRA) and denitrification) and two oxidation pathways (nitrification and anaerobic ammonium oxidation (anammox)) (Delwiche, 1970). We found that all four reduction pathways of nitrogen cycle existed in CAs (Fig. S4A). Then, we mapped the available reference genomes of *Microcystis* and *Dolichospermum* from NCBI into the nitrogen metabolism of KEGG. Only one module (ANRA) of the nitrogen cycle was found in the *Microcystis* genome and two (ANRA and nitrogen fixation) in the *Dolichospermum* genome. More specifically, DNRA and denitrification occurred only in the bacteria, suggesting that cyanobacteria and their attached bacteria formed nitrogen-cycling co-pathways.

To identify other candidate bacterial participants in the nitrogen cycle, we performed binning analysis with CONCOCT and obtained 8 "High quality drafts" (≥90% complete and <5% contamination) and 43 'Medium-quality drafts' (≥50% and <10% contamination)(Bowers et al., 2017). By mapping these 51 genomes to the nitrogen cycle, we captured the bacteria that were potential participants in the nitrogen cycle and constructed a nitrogen co-pathway with candidate participants for different modules (Fig. 6). The results showed that *Microcystis acruginosa* and *Dolichospermum flos-aquae* participated in ANRA, *Alistipes indistinctus* participates in DNRA, *Proteobacteria bacterium JGI* in denitrification, and *Dolichospermum flos-aquae* in nitrogen fixation.

To characterize the dynamics of nitrogen metabolism in CAs, we compared nitrogen metabolism-related genes in MCA with that in DCA using the Wilcoxon rank-sum tests. We found that five genes were significantly enriched and four genes were significantly deficient in MCA, compared to DCA ($P < 0.05$) (Fig. S4B). DNRA module that can transform nitrate nitrogen to biologically available ammonium was enriched in MCA, indicating the excessive production of ammonium in MCA. The synthesis of L-glutamine from ammonia was also significantly promoted in MCA, which was most likely resulted from the mass propagation and growth of the cyanobacteria during heavy blooming.

4. Discussion

The Lake Taihu blooms showed seasonal dynamics, as demonstrated by alternate succession of dominant cyanobacterial genera between *Microcystis* and *Dolichospermum*. In the current study, 40 μm Cell Strainers was used to collect CAs. Most of the *Synechococcus* cells would be filtered out during the sampling. This did not cause any systematic biases in the study of the relationship between cyanobacterial aggregate and bacteria because only *Microcystis* and *Dolichospermum* formed large-size aggregates. This is also proved by our results (Fig. 1B) that the CAs was dominated by only *Microcystis* and *Dolichospermum*. Total nitrogen, total phosphorus and water temperature were three dominant factors influencing the alternate succession. This corroborates previous findings of successions of dominant cyanobacteria between different genera or different *Microcystis* spp.

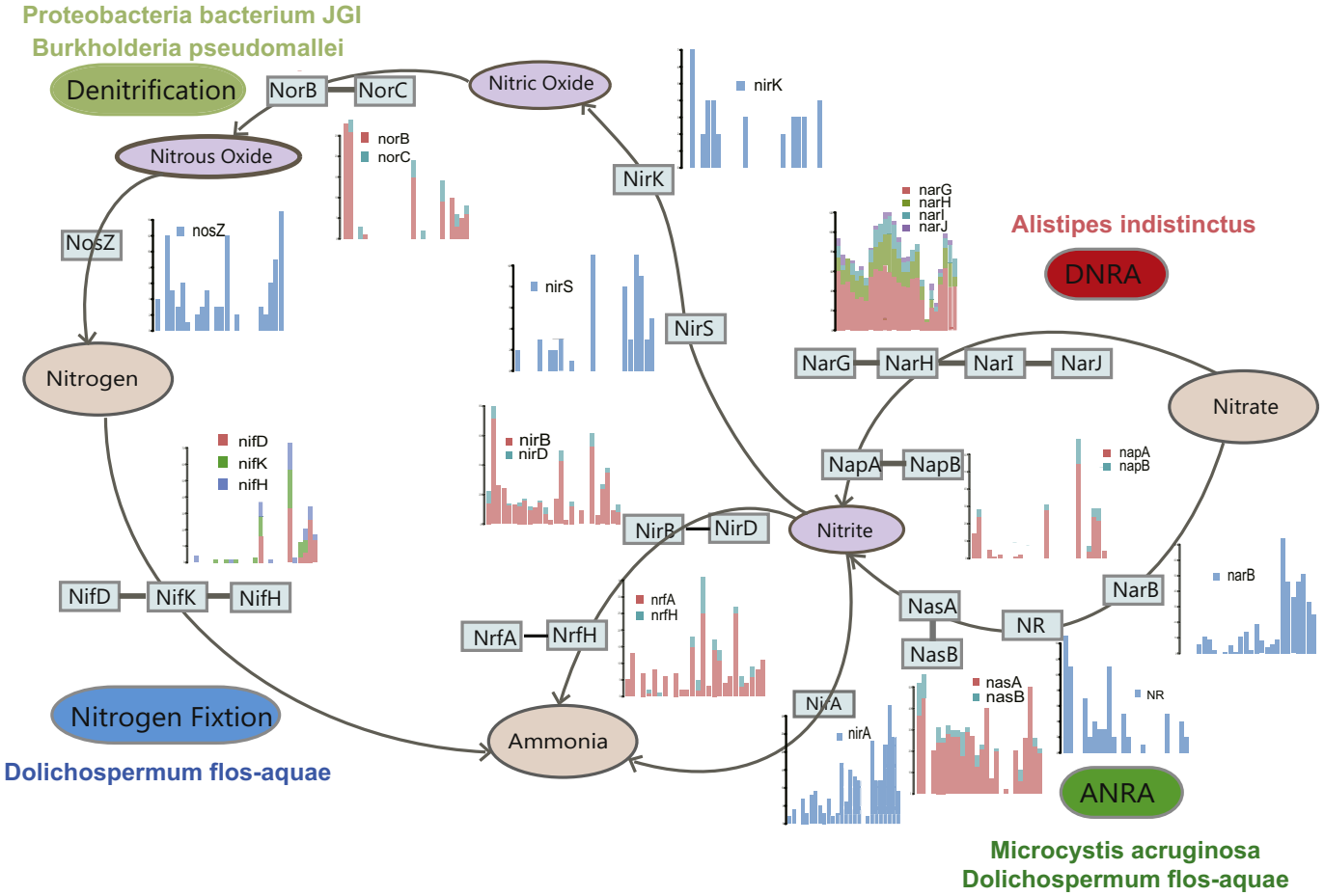

Fig. 6. Nitrogen co-pathways between cyanobacteria and their attached bacteria. Ellipses represent the formations of nitrogen in CAs. Four rounded rectangles colored light green represent four reduction modules (nitrogen fixation, ANRA-assimilatory nitrate reduction, DNRA-dissimilatory nitrate reduction and denitrification). The rectangles colored light blue represent the functional genes linked to nitrogen cycling identified in the CAs, and the bar plot near them represents their abundance. Mapping reference genome of *Microcystis* and *Dolichospermum* to nitrogen modules showed that only the ANRA module was involved in *Microcystis* and that ANRA and nitrogen fixation were involved in *Dolichospermum*. DNRA and denitrification occurred only in the bacteria. Only partial modules of nitrogen cycle were involved in *Microcystis and Dolichospermum*, and a nearly complete nitrogen pathway appeared in CA samples, indicating that cyanobacteria and their attached bacteria formed nitrogen co-pathways.

recorded in Lake Taihu and other water ecosystems (Fernández et al., 2015a; Niu et al., 2011; Pechal et al., 2014; Wu et al., 2010a; Zhang et al., 2014). Previous studies showed *Microcystis* aggregates dominated the period of heavy cyanobacterial blooming in summer and autumn (Dziallas and Grossart, 2011; Fiore et al., 2013; Liu et al., 2014). In laboratory studies, *Microcystis* and *Dolichospermum* isolated from Lake Taihu were shown to have interspecies competition with co-cultivation (Zhang et al., 2014). Also, studies of Dianchi Lake showed that temperature, total nitrogen and total phosphorus along alternate succession were most correlated to *Aphanizomenon flos-aquae* and *Microcystis aeruginosa* (Wu et al., 2010a). In a hypereutrophic drinking water supply reservoir, total phosphorus level and parameters related to seasonality, *i.e.*, temperature and solar radiation, were found to trigger cyanobacterial dominance and succession between *Microcystis natans* and *Anabaena circinalis* (Fernández et al., 2015a). These findings suggest that alternate succession of different cyanobacterial genera or species may be a prevalent phenomenon during cyanobacterial blooms and that such successions are driven mainly by environmental factors, such as water temperature and nutrient concentrations.

Total nitrogen and total phosphorus showed high positive correlation (Fig. S2C). When total nitrogen and total phosphorus were high, the *Dolichospermum* dominated the CAs (Fig. S2B). Phosphorus enrichment was suggested to facilitate dinitrogen fixation (Wang et al., 2018), which may explain the high abundance of *Dolichospermum* in CAs. Community composition of *Dolichospermum*-dominated CAs with high total nitrogen and total phosphorus showed significantly lower diversity than that of *Microcystis*-dominated CAs, which is consistent with the resource-ratio theory, "more resource, less diversity" (Tilman, 1982). The resource-ratio theory was tested in a microbial community in laboratory cultures (Hibbing et al., 2010). The rRNA operon copy number was demonstrated to be a proxy genomic signature for one of the various ecological strategies that bacteria exhibit by cultivation study (Lauro et al., 2009) and community study (Wu et al., 2017). The average rRNA operon copy number decreased over time in ecological succession, which was indirectly associated with changes in resource availability (Nemergut et al., 2016). Here, we showed that the average rRNA copy number was higher under high total nitrogen levels, and we discovered a high positive correlation between copy number and total nitrogen.

Our analyses revealed that the attached bacteria were more correlated with cyanobacteria than with the environment. The relationship between cyanobacteria and their attached bacteria was previously investigated by (Komárková et al., 2010; Peng et al., 2007; Wilhelm et al., 2011), all of whom suggested a high degree of correlation between bacteria and cyanobacteria community compositions. Here, our ecological network analyses revealed the small world around *Dolichospermum* and *Microcystis*. This microcosm property, which was suggested to make the community more robust to perturbations, was reported in marine microbes (Montoya et al., 2006). However, most bacteria in the aggregates of *Dolichospermum* and *Microcystis* were not found in existing genome database, revealing our limited knowledge on cyanobacteria-associated bacteria. One neighbor of *Dolichospermum* discovered by ecological network analyses was *Burkholderia*, which was reported to coexist with cyanobacteria (Wolinska et al., 2017). Genome annotation of *Burkholderia* species showed that many species of *Burkholderia*, such as *Burkholderia pseudomallei*, *Burkholderia mallei* and *Burkholderia thailandensis*, can perform denitrification (Wiersinga et al., 2006) and thus could be correlated with *Dolichospermum* through nitrogen pathways. *Dechloromonas*, closely associated to *Microcystis*, has a large number of environmental sensors and signaling pathways (Salinero et al., 2009). Two *Dechloromonas* strains were also reported to completely mineralize various mono-aromatic compounds with nitrate as the electron acceptor (Coates et al., 2001). These results indicate the importance of the nitrogen pathway as a functional link by which to form mutualistic relationships between cyanobacteria and their closely attached bacteria. Nitrogen has also been widely reported as one of the most important factors affecting CyanoHABs in culture-based experiments (Beversdorf et al., 2013; Chaffin and Bridgeman, 2014; Conley et al., 2009; Paerl et al., 2014; Yu et al., 2014). However, few studies have been carried out to determine the co-participators in the nitrogen cycle within cyanobacteria aggregates. Here, our metagenomic analyses suggest that cyanobacteria and bacteria potentially co-participate in the nitrogen cycle.

Some well-known relationships, such as suspended solids and turbidity (Spearman' correlation 0.89), or algae cell density and chlorophyll *a* (0.94), were reported. Both partial Mantel tests and SEM analysis showed that the attached bacterial composition was more correlated with the cyanobacterial composition than with the environmental factors. Previous studies also concluded that environment-mediated alternate succession of cyanobacteria likely shaped the variations of their attached bacteria (Niu et al., 2011). Nutrient concentration may directly influence the bacteria in CAs by affecting bacterial growth (Haukka et al., 2006; Pinhassi and Hagström, 2000). However, bacterial community was more related to cyanobacteria than environmental factors in our study. It is possible that nutrients may have an indirect impact on bacteria through their influence on cyanobacterial populations.

Water pollution, as affected by supplemented nutrients, is a fundamental problem that can result in the imbalance of complex freshwater ecosystems composed of multiple interacting microbial groups. Documented global increase in the frequency and persistence of blooms of cyanobacteria continues to alarm researchers and environmental managers. Consistent with previous studies in Lake Taihu and many lakes worldwide, this study demonstrates that two cyanobacteria genera (*Dolichospermum* and *Microcystis*) could be characterized by alternate succession of CAs in different seasons in a manner dependent on changes in temperature and nutrient supply. Mutualistic relationships were discovered between cyanobacteria and their closely attached bacteria, both from ecological network analysis at the taxonomic level and co-pathway analysis at the gene level. With these results, we discovered a co-dependency of CA constituents. Further research on codependency between attached bacteria and cyanobacteria may offer potential targets for controlling toxic blooms.

5. Conclusions

While the attached bacteria have been reported to be indispensable for the cyanobacteria to form the organization of aggregates during CyanoHABs, it is still not clear what the role the cyanobacteria and their attached bacteria are playing for the microbial ecology of the CAs. Mutualistic relationships are assumed to exist between bacteria and cyanobacteria in these CAs. Here, we observed the alternate succession of two cyanobacteria genera (*Microcystis* and *Dolichospermum*) by the semi-quantitative *in vivo* monitor and elucidated the significantly different bacterial community attached to *Microcystis* and *Dolichospermum* by 16S rRNA analysis. Besides, the bacterial community was found to be more correlated to the cyanobacterial community than to the environmental factors. A potential co-dependent nitrogen-cycling pathway between cyanobacteria and their attached bacteria, a critical functional link within the community, was constructed. Overall, these results demonstrated that mutualistic relationships do, indeed, exist between cyanobacteria and bacteria in CAs at both taxonomic and gene levels, providing biological clues potentially leading to the control of blooms by interventional strategies to disrupt bacteria-cyanobacteria relationships and co-pathways.

Supplementary data to this article can be found online at https://doi.org/10.1016/j.scitotenv.2019.06.150.

Declaration of Competing Interest

The authors declare that they have no known competing financial interests or personal relationships that could have appeared to influence the work reported in this paper.

Acknowledgements

This research was supported by the National Natural Science Foundation of China (Grant NO. 61561146396, 61721003, 61322308, 61673241, 61872218, 31600096), and Tsinghua-Fuzhou Institute research program, Beijing National Research Center for Information Science and Technology. The funders had no role in study design, data collection and analysis, decision to publish, or preparation of the manuscript.

References

Alneberg, J., Bjarnason, B.S., De Bruijn, I., Schirmer, M., Quick, J., Ijaz, U.Z., et al., 2014. Binning metagenomic contigs by coverage and composition. Nat. Methods 11, 1144–1146.
Andersson, A.F., Riemann, L., Bertilsson, S., 2010. Pyrosequencing reveals contrasting seasonal dynamics of taxa within Baltic Sea bacterioplankton communities. ISME J. 4, 171–181.
Assenov, Y., Ramírez, F., Schelhorn, S.-E., Lengauer, T., Albrecht, M., 2007. Computing topological parameters of biological networks. Bioinformatics 24, 282–284.
Bbosa, N.B., Oyoo, W.S., 2013. Seasonal variations of phytoplankton species in Lake Victoria and the influence of iron and zinc ions on the dominant species identified during 2006–2007 studies. Lakes Reserv. Res. Manag. 18, 259–273.
Berg, K.A., Lyra, C., Sivonen, K., Paulin, L., Suomalainen, S., Tuomi, P., et al., 2009. High diversity of cultivable heterotrophic bacteria in association with cyanobacterial water blooms. ISME J 3, 314–325.
Beversdorf, L.J., Miller, T.R., McMahon, K.D., 2013. The role of nitrogen fixation in cyanobacterial bloom toxicity in a temperate, eutrophic lake. PLoS One 8, e56103.
Bowers, R.M., Kyrpides, N.C., Stepanauskas, R., Harmon-Smith, M., Doud, D., Reddy, T., et al., 2017. Minimum information about a single amplified genome (MISAG) and a metagenome-assembled genome (MIMAG) of bacteria and archaea. Nat. Biotechnol. 35, 725–731.
Brookes, J.D., Ganf, G.G., Green, D., Whittington, J., 1999. The influence of light and nutrients on buoyancy, filament aggregation and flotation of Anabaena circinalis. Am. J. Kidney Dis. 21, 327–341.
Buchfink, B., Xie, C., Huson, D.H., 2015. Fast and sensitive protein alignment using DIAMOND. Nat Meth 12, 59–60.
Cai, H.Y., Yan, Z.S., Wang, A.J., Krumholz, L.R., Jiang, H.L., 2013a. Analysis of the attached microbial community on mucilaginous cyanobacterial aggregates in the eutrophic Lake Taihu reveals the importance of Planctomycetes. Microb. Ecol. 66, 73–83.
Cai, H.Y., Yan, Z.S., Wang, A.J., Krumholz, L.R., Jiang, H.L., 2013b. Analysis of the attached microbial community on mucilaginous cyanobacterial aggregates in the eutrophic Lake Taihu reveals the importance of Planctomycetes. Microb. Ecol. 66, 73–83.
Cai, H., Jiang, H., Krumholz, L.R., Yang, Z., 2014. Bacterial community composition of size-fractioned aggregates within the phycosphere of cyanobacterial blooms in a eutrophic freshwater lake. PLoS One 9, e102879.
Callieri, C., Lami, A., Bertoni, R., 2011. Microcolony formation by single-cell Synechococcus strains as a fast response to UV radiation. Applied & Environmental Microbiology 77, 7533–7540.
Caporaso, J.G., Kuczynski, J., Stombaugh, J., Bittinger, K., Bushman, F.D., Costello, E.K., et al., 2010. QIIME allows analysis of high-throughput community sequencing data. Nat. Methods 7, 335–336.
Chaffin, J.D., Bridgeman, T.B., 2014. Organic and inorganic nitrogen utilization by nitrogen-stressed cyanobacteria during bloom conditions. J. Appl. Phycol. 26, 299–309.
Chen, Y., Qin, B., Teubner, K., Dokulil, M.T., 2003a. Long-term dynamics of phytoplankton assemblages : Microcystis-domination in Lake Taihu, a large shallow lake in China. J. Plankton Res. 25 (9), 445–453.
Chen, Y., Qin, B., Teubner, K., Dokulil, M.T., 2003b. Long-term dynamics of phytoplankton assemblages: Microcystis-domination in Lake Taihu, a large shallow lake in China. J. Plankton Res. 25, 445–453.
Cheung, M.Y., Liang, S., Lee, J., 2013. Toxin-producing cyanobacteria in freshwater: a review of the problems, impact on drinking water safety, and efforts for protecting public health. J. Microbiol. 51, 1–10.
Coates, J.D., Chakraborty, R., Lack, J.G., Oconnor, S.M., Cole, K.A., Bender, K.S., et al., 2001. Anaerobic benzene oxidation coupled to nitrate reduction in pure culture by two strains of Dechloromonas. Nature 411, 1039–1043.
Conley, D.J., Paerl, H.W., Howarth, R.W., 2009. Controlling eutrophication: nitrogen and phosphorus. Science 323, 1014 H.W.Wilson - GS.
Davis, T.W., Berry, D.L., Boyer, G.L., Gobler, C.J., 2009. The effects of temperature and nutrients on the growth and dynamics of toxic and non-toxic strains of Microcystis during cyanobacteria blooms. Harmful Algae 8, 715–725.
Delwiche, C.C., 1970. The nitrogen cycle. Sci. Am. 223, 136–147.
Deng, Y., Jiang, Y.-H., Yang, Y., He, Z., Luo, F., Zhou, J., 2012. Molecular ecological network analyses. BMC bioinformatics 13, 113.
Desantis, T.Z., Hugenholtz, P., Larsen, N., Rojas, M., Brodie, E.L., Keller, K., et al., 2006. Greengenes, a chimera-checked 16S rRNA gene database and workbench compatible with ARB. Applied & Environmental Microbiology 72, 5069–5072.
Ding, J.Q., Zhang, J.Y., 2011. Application of YSI 6600 for Cyanobacteria Bloom Early Warning in Taihu Lake. Administration & Technique of Environmental Monitoring.
Dziallas, C., Grossart, H.P., 2011. Temperature and biotic factors influence bacterial communities associated with the cyanobacterium Microcystis sp. Environ. Microbiol. 13, 1632–1641.
Falony, G., Joossens, M., Vieira-Silva, S., Wang, J., Darzi, Y., Faust, K., et al., 2016. Population-level analysis of gut microbiome variation. Science 352, 560–564.
Fernández, C., Estrada, V., Parodi, E.R., 2015a. Factors triggering cyanobacteria dominance and succession during blooms in a hypereutrophic drinking water supply reservoir. Water Air Soil Pollut. 226, 73.
Fernández, C., Estrada, V., Parodi, E.R., 2015b. Factors triggering cyanobacteria dominance and succession during blooms in a hypereutrophic drinking water supply reservoir. Water Air Soil Pollut. 226, 1–13.
Fiore, M.F., Alvarenga, D.O., Varani, A.M., Hoff-Risseti, C., Crespim, E., Ramos, R.T., et al., 2013. Draft genome sequence of the Brazilian toxic bloom-forming cyanobacterium Microcystis aeruginosa strain SPC777. Genome Announc 1.
Grant, M.A., Kazamia, E., Cicuta, P., Smith, A.G., 2014. Direct exchange of vitamin B12 is demonstrated by modelling the growth dynamics of algal-bacterial cocultures. ISME J. 8, 1418–1427.
Guo, L., 2007. Ecology. Doing battle with the green monster of Taihu Lake. Science 317, 1166.
Hai, X., Paerl, H.W., Qin, B., Zhu, G., Guang, G., 2010. Nitrogen and phosphorus inputs control phytoplankton growth in eutrophic Lake Taihu, China. Limnology & Oceanography 55, 420–432.
Haukka, K., Kolmonen, E., Hyder, R., Hietala, J., Vakkilainen, K., Kairesalo, T., et al., 2006. Effect of nutrient loading on bacterioplankton community composition in lake mesocosms. Microb. Ecol. 51, 137–146.
Havens, K.E., 2008. Cyanobacteria blooms: effects on aquatic ecosystems. Adv. Exp. Med. Biol. 619, 733–747.
Hibbing, M.E., Fuqua, C., Parsek, M.R., Peterson, S.B., 2010. Bacterial competition: surviving and thriving in the microbial jungle. Nat. Rev. Microbiol. 8, 15–25.
Hultman, J., Waldrop, M.P., Mackelprang, R., David, M.M., McFarland, J., Blazewicz, S.J., et al., 2015. Multi-omics of permafrost, active layer and thermokarst bog soil microbiomes. Nature 521, 208–212.
Huson, D.H., Auch, A.F., Qi, J., Schuster, S.C., 2007. MEGAN analysis of metagenomic data. Genome Res. 17, 377–386.
Hyatt, D., LoCascio, P.F., Hauser, L.J., Uberbacher, E.C., 2012. Gene and translation initiation site prediction in metagenomic sequences. Bioinformatics 28, 2223–2230.
Kanehisa, M., Goto, S., Kawashima, S., Okuno, Y., Hattori, M., 2004. The KEGG resource for deciphering the genome. Nucleic Acids Res. 32, D277–D280.
Kanungo, T., Mount, D.M., Netanyahu, N.S., Piatko, C.D., Silverman, R., Wu, A.Y., 2002. An efficient k-means clustering algorithm: analysis and implementation. IEEE Trans. Pattern Anal. Mach. Intell. 24, 881–892.
Kara, E.L., Hanson, P.C., Hu, Y.H., Winslow, L., McMahon, K.D., 2013. A decade of seasonal dynamics and co-occurrences within freshwater bacterioplankton communities from eutrophic Lake Mendota, WI, USA. ISME J 7, 680–684.
Kiage, L.M., Walker, N.D., 2009. Using NDVI from MODIS to monitor duckweed bloom in Lake Maracaibo, Venezuela. Water Resour. Manag. 23, 1125–1135.
Komárková, J., Jezberová, J., Komárek, O., Zapomělová, E., 2010. Variability of Chroococcus (Cyanobacteria) morphospecies with regard to phylogenetic relationships. Hydrobiologia 639, 69–83.
Lauro, F.M., Mcdougald, D., Thomas, T., Williams, T.J., Egan, S., Rice, S., et al., 2009. The genomic basis of trophic strategy in marine bacteria. Proc. Natl. Acad. Sci. U. S. A. 106, 15527–15533.
Li, D., Liu, C.M., Luo, R., Sadakane, K., Lam, T.W., 2015. MEGAHIT: an ultra-fast single-node solution for large and complex metagenomics assembly via succinct de Bruijn graph. Bioinformatics 31, 1674–1676.
Lima-Mendez, G., Faust, K., Henry, N., Decelle, J., Colin, S., Carcillo, F., et al., 2015. Ocean plankton. Determinants of community structure in the global plankton interactome. Science 348, 1262073.
Liu, Z.Z., Zhu, J.P., Li, M., Xue, Q.Q., Zeng, Y., Wang, Z.P., 2014. Effects of freshwater bacterial siderophore on Microcystis and Anabaena. Biol. Control 78, 42–48.
Montoya, J.M., Pimm, S.L., Solé, R.V., 2006. Ecological networks and their fragility. Nature 442, 259–264.
Mootha, V.K., Lindgren, C.M., Eriksson, K.F., Subramanian, A., Sihag, S., Lehar, J., et al., 2003. PGC-1alpha-responsive genes involved in oxidative phosphorylation are coordinately downregulated in human diabetes. Nat. Genet. 34, 267–273.
Mou, X.Z., Jacob, J., Lu, X.X., Robbins, S., Sun, S.L., Ortiz, J.D., 2013. Diversity and distribution of free-living and particle-associated bacterioplankton in Sandusky Bay and adjacent waters of Lake Erie Western Basin. J. Great Lakes Res. 39, 352–357.
Nemergut, D.R., Knelman, J.E., Scott, F., Teresa, B., Brett, M., Lin, J., et al., 2016. Decreases in average bacterial community rRNA operon copy number during succession. ISME J. 10, 1147.
Niu, Y., Shen, H., Chen, J., Xie, P., Yang, X., Tao, M., et al., 2011. Phytoplankton community succession shaping bacterioplankton community composition in Lake Taihu, China. Water Res. 45, 4169–4182.
O'Hara, R.B., Legendre, P., Stevens, M.H., Blanchet, F.G., Kindt, R., Solymos, P., et al., 2011. Vegan: community ecology package. Version 2.0-2. J. Stat. Softw. 48, 1–21.
Otten, T.G., Paerl, H.W., 2011. Phylogenetic inference of colony isolates comprising seasonal microcystis blooms in Lake Taihu, China. Microb. Ecol. 62, 907–918.
Overbeek, R., Begley, T., Butler, R.M., Choudhuri, J.V., Chuang, H.Y., Cohoon, M., et al., 2005. The subsystems approach to genome annotation and its use in the project to annotate 1000 genomes. Nucleic Acids Res. 33, 5691–5702.
Paerl, H.W., Huisman, J., 2008. Blooms like it hot. Science 320, 57–58.
Paerl, H.W., Gardner, W.S., Mccarthy, M.J., Peierls, B.L., Wilhelm, S.W., 2014. Algal blooms: noteworthy nitrogen. Science 346, 175.
Parks, D.H., Imelfort, M., Skennerton, C.T., Hugenholtz, P., Tyson, G.W., 2015. CheckM: assessing the quality of microbial genomes recovered from isolates, single cells, and metagenomes. Genome Res. 25, 1043–1055.
Pechal, J.L., Crippen, T.L., Benbow, M.E., Tarone, A.M., Dowd, S., Tomberlin, J.K., 2014. The potential use of bacterial community succession in forensics as described by high throughput metagenomic sequencing. Int. J. Legal Med. 128, 193–205.

Peng, X., Fanxiang, K., Huansheng, C., Min, Z., 2007. Relationship between bacterioplankton and phytoplankton community dynamics during late spring and early summer in Lake Taihu, China. Acta Ecol. Sin. 27, 1696–1702.
Pinhassi, J., Hagström, Å., 2000. Seasonal succession in marine bacterioplankton. Aquat. Microb. Ecol. 21, 245–256.
Qin, B., Xu, P., Wu, Q., Luo, L., Zhang, Y., 2007. Environmental issues of Lake Taihu, China. Hydrobiologia 581, 3–14.
Quinlan, A.R., Hall, I.M., 2010. BEDTools: a flexible suite of utilities for comparing genomic features. Bioinformatics 26, 841–842.
Rondon, M.R., August, P.R., Bettermann, A.D., Brady, S.F., Grossman, T.H., Liles, M.R., et al., 2000. Cloning the soil metagenome: a strategy for accessing the genetic and functional diversity of uncultured microorganisms. Appl. Environ. Microbiol. 66, 2541–2547.
Rosseel, Y., 2015. lavaan: latent variable analysis. Infection & Immunity 63, 2403–2408.
Salinero, K.K., Keller, K., Feil, W.S., Feil, H., Trong, S., Bartolo, G.D., et al., 2009. Metabolic analysis of the soil microbe Dechloromonas aromatica str. RCB: indications of a surprisingly complex life-style and cryptic anaerobic pathways for aromatic degradation. BMC Genomics 10, 351.
Salomonson, V.V., Barnes, W., Maymon, P.W., Montgomery, H.E., Ostrow, H., 1989. MODIS: advanced facility instrument for studies of the Earth as a system. IEEE Trans. Geosci. Remote Sens. 27, 145–153.
Shi, L., Cai, Y., Kong, F., Yu, Y., 2012a. Specific association between bacteria and buoyant Microcystis colonies compared with other bulk bacterial communities in the eutrophic Lake Taihu, China. Environ. Microbiol. Rep. 4, 669–678.
Shi, L., Cai, Y., Kong, F., Yu, Y., 2012b. Specific association between bacteria and buoyant Microcystis colonies compared with other bulk bacterial communities in the eutrophic Lake Taihu, China. Environ. Microbiol. Rep. 4, 669–678.
Shi, K., Zhang, Y., Zhou, Y., Liu, X., Zhu, G., Qin, B., et al., 2017. Long-term MODIS observations of cyanobacterial dynamics in Lake Taihu: responses to nutrient enrichment and meteorological factors. Sci. Rep. 7, 40326.
Simpson, G.L., Solymos, P., Stevens, M., Wagner, H., 2015. Vegan: community ecology package. Time International 1997, 15–17.
Smith, A.D., Gilbert, J.J., 2010. Spatial and temporal variability in filament length of a toxic cyanobacterium (Anabaena affinis). Freshw. Biol. 33, 1–11.
Sommer, U., 1989. Nutrient status and nutrient competition of phytoplankton in a shallow, hypertrophic lake. Limnology & Oceanography 34, 1162–1173.
State Environmental Protection Administration of China, 2002. Water and Wastewater Monitoring and Analysis Methods. 4th Ed. China Environmental Science Press, Beijing, pp. 210–213.
Stoddard, S.F., Smith, B.J., Hein, R., Roller, B.R., Schmidt, T.M., 2015. rrnDB: improved tools for interpreting rRNA gene abundance in bacteria and archaea and a new foundation for future development. Nucleic Acids Res. 43, D593–D598.
Subramanian, A., Tamayo, P., Mootha, V.K., Mukherjee, S., Ebert, B.L., Gillette, M.A., et al., 2005. Gene set enrichment analysis: a knowledge-based approach for interpreting genome-wide expression profiles. Proc. Natl. Acad. Sci. U. S. A. 102, 15545–15550.
Sunagawa, S., Coelho, L.P., Chaffron, S., Kultima, J.R., Labadie, K., Salazar, G., et al., 2015. Ocean plankton. Structure and function of the global ocean microbiome. Science 348, 1261359.
Tang, X., Gao, G., Qin, B., Zhu, L., Chao, J., Wang, J., et al., 2009. Characterization of bacterial communities associated with organic aggregates in a large, shallow, eutrophic freshwater lake (Lake Taihu, China). Microb. Ecol. 58, 307–322.
Tilman, D., 1982. Resource competition and community structure. Monogr. Popul. Biol. 17, 1.
Tyson, G.W., Chapman, J., Hugenholtz, P., Allen, E.E., Ram, R.J., Richardson, P.M., et al., 2004. Community structure and metabolism through reconstruction of microbial genomes from the environment. Nature 428, 37–43.
Vézie, C., Rapala, J., Vaitomaa, J., Seitsonen, J., Sivonen, K., 2002. Effect of nitrogen and phosphorus on growth of toxic and nontoxic Microcystis strains and on intracellular microcystin concentrations. Microb. Ecol. 43, 443–454.
Wang, Y., Chen, F., 2008. Decomposition and phosphorus release from four different size fractions of Microcystis spp. taken from Lake Taihu, China. J. Environ. Sci. 20, 891–896.
Wang, X., Sun, M., Xie, M., Liu, M., Luo, L., Li, P., et al., 2013. Differences in microcystin production and genotype composition among Microcystis colonies of different sizes in Lake Taihu. Water Res. 47, 5659–5669.
Wang, S., Xiao, J., Wan, L., Zhou, Z., Wang, Z., Song, C., et al., 2018. Mutual Dependence of Nitrogen and Phosphorus as Key Nutrient Elements: One Facilitates Dolichospermum Flos-aquae to Overcome the Limitations of the Other. p. 52 (acs.est.7b04992).
Wiersinga, W.J., Van, dPT, White, N.J., Day, N.P., Peacock, S.J., 2006. Melioidosis: insights into the pathogenicity of Burkholderia pseudomallei. Nat. Rev. Microbiol. 4, 272–282.
Wilhelm, S.W., Farnsley, S.E., LeCleir, G.R., Layton, A.C., Satchwell, M.F., DeBruyn, J.M., et al., 2011. The relationships between nutrients, cyanobacterial toxins and the microbial community in Taihu (Lake Tai), China. Harmful Algae 10, 207–215.
Wolinska, A., Kuzniar, A., Zielenkiewicz, U., Banach, A., Izak, D., Stepniewska, Z., et al., 2017. Metagenomic analysis of some potential nitrogen-fixing bacteria in arable soils at different formation processes. Microb. Ecol. 73, 162–176.
Wooley, J.C., Godzik, A., Friedberg, I., 2010. A primer on metagenomics. PLoS Comput. Biol. 6, e1000667.
Worm, J., Søndergaard, M., 1998. Dynamics of heterotrophic bacteria attached to Microcystis spp. (Cyanobacteria). Aquat. Microb. Ecol. 14, 19–28.
Wu, W., Li, G., Li, D., Liu, Y., 2010a. Temperature may be the dominating factor on the alternant succession of Aphanizomenon flos-aquae and Microcystis aeruginosa in Dianchi Lake. Fresenius Environ. Bull. 20, 846–853.
Wu, W., Li, G., Li, D., Liu, Y., 2010b. Temperature may be the dominating factor on the alternant succession of Aphanizomenon flos-aquae and Microcystis aeruginosa in Dianchi Lake. Fresenius Environ. Bull. 19, 846–853.
Wu, Y., Li, L., Gan, N., Zheng, L., Ma, H., Shan, K., et al., 2014. Seasonal dynamics of water bloom-forming Microcystis morphospecies and the associated extracellular microcystin concentrations in large, shallow, eutrophic Dianchi Lake. J. Environ. Sci. (China) 26, 1921–1929.
Wu, L., Yang, Y., Chen, S., Jason Shi, Z., Zhao, M., Zhu, Z., et al., 2017. Microbial functional trait of rRNA operon copy numbers increases with organic levels in anaerobic digesters. Isme j 11, 2874–2878.
Yao, Z., Wang, A., Li, Y., Cai, Z., Lemaitre, B., Zhang, H., 2016. The dual oxidase gene BdDuox regulates the intestinal bacterial community homeostasis of Bactrocera dorsalis. Isme j 10, 1037–1050.
Ye, W., Tan, J., Liu, X., Lin, S., Pan, J., Li, D., et al., 2011. Temporal variability of cyanobacterial populations in the water and sediment samples of Lake Taihu as determined by DGGE and real-time PCR. Harmful Algae 10, 472–479.
Ying, A., Bi, Y., Hu, Z., 2015. Response of predominant phytoplankton species to anthropogenic impacts in Lake Taihu. J. Freshw. Ecol. 30, 99–112.
Yu, G., Jiang, Y., Song, G., Tan, W., Zhu, M., Li, R., 2014. Variation of Microcystis and microcystins coupling nitrogen and phosphorus nutrients in Lake Erhai, a drinking-water source in Southwest Plateau, China. Environ. Sci. Pollut. Res. 21, 9887–9898.
Zhang, P., Zhai, C., Chen, R., Liu, C., Xue, Y., Jiang, J., 2012. The dynamics of the water bloom-forming Microcystis aeruginosa and its relationship with biotic and abiotic factors in Lake Taihu, China. Ecol. Eng. 47, 274–277.
Zhang, X.W., Fu, J., Song, S., Zhang, P., Yang, X.H., Zhang, L.R., et al., 2014. Interspecific competition between Microcystis aeruginosa and Anabaena flos-aquae from Taihu Lake, China. Z. Naturforsch. C 69, 53–60.
Zhang, J., Zhu, C., Guan, R., Xiong, Z., Zhang, W., Shi, J., et al., 2017. Microbial profiles of a drinking water resource based on different 16S rRNA V regions during a heavy cyanobacterial bloom in Lake Taihu, China. Environ. Sci. Pollut. Res. Int. 24, 12796–12808.
Zhernakova, A., Kurilshikov, A., Bonder, M.J., Tigchelaar, E.F., Schirmer, M., Vatanen, T., et al., 2016. Population-based metagenomics analysis reveals markers for gut microbiome composition and diversity. Science 352, 565–569.
Zhou, J., Deng, Y., Luo, F., He, Z., Tu, Q., Zhi, X., 2010. Functional molecular ecological networks. MBio 1 (e00169-10).
Zhou, J., Deng, Y., Luo, F., He, Z., Yang, Y., 2011. Phylogenetic molecular ecological network of soil microbial communities in response to elevated CO_2. MBio 2 (e00122-11).
Zhu, B.C., Zhang, J.Y., Wei, K., Huang, J., Song, T., Zhi-Jian, W.U., 2011. Application of semi-quantitative vivo monitoring method for phytoplankton in cyanobacteria blooms forewarning. Environmental Monitoring & Forewarning 3, 8–11.
Zhu, W., Zhou, X., Chen, H., Gao, L., Xiao, M., Li, M., 2016. High nutrient concentration and temperature alleviated formation of large colonies of Microcystis: evidence from field investigations and laboratory experiments. Water Research 101, 167–175.